

Strain-induced shift in the elastically soft direction of epitaxially grown fcc metals

V. Ozolinš, C. Wolverton, and Alex Zunger
National Renewable Energy Laboratory, Golden, CO 80401
(October 20, 1997)

The theory of epitaxial strain energy is extended beyond the harmonic approximation to account for large film/substrate lattice mismatch. We find that for fcc noble metals (i) directions $\langle 001 \rangle$ and $\langle 111 \rangle$ soften under *tensile* biaxial strain (unlike zincblende semiconductors) while (ii) $\langle 110 \rangle$ and $\langle 201 \rangle$ soften under *compressive* biaxial strain. Consequently, (iii) upon sufficient compression $\langle 201 \rangle$ becomes the softest direction (lowest elastic energy), but (iv) $\langle 110 \rangle$ is the hardest direction for large tensile strain. (v) The dramatic softening of $\langle 001 \rangle$ in fcc noble metals upon biaxial tensile strain is caused by small fcc/bcc energy differences for these materials. These results can be used in selecting the substrate orientation for effective epitaxial growth of pure elements and A_pB_q superlattices, as well as to explain the shapes of coherent precipitates in phase separating alloys.

PACS numbers: 62.20.Dc, 68.60.-p, 81.10.Aj

When a material is compressed *hydrostatically*, its energy rises steeply because all three crystal axes are deformed (dashed line in Fig. 1). When the same material is confined coherently onto a substrate (“coherent epitaxy”) with lattice constant a_s , the energy rises less steeply (solid line in Fig. 1) since it is deformed only along the crystal axes in the substrate plane and allowed to relax (and thus, lower its energy) in the third direction \hat{G} . This “epitaxial softening” can be quantified by the dimensionless parameter

$$q(a_s, \hat{G}) = \frac{\Delta E^{\text{epi}}(a_s, \hat{G})}{\Delta E^{\text{bulk}}(a_s)}, \quad (1)$$

giving the ratio between the epitaxial increase in energy due to biaxial deformation to a_s , and the hydrostatic increase in energy due to triaxial deformation to the same a_s . Because the biaxial strain energy $\Delta E^{\text{epi}}(a_s, \hat{G})$ depends on the strain direction \hat{G} , so does $q(a_s, \hat{G})$. In growing coherent epitaxial films,¹ it is desirable to minimize $\Delta E^{\text{epi}}(a_s, \hat{G})$ [or, equivalently, for a fixed a_s minimize $q(a_s, \hat{G})$], so as to avoid or reduce dislocations and other strain-induced film/substrate defects. It is hence important to select substrates a_s and growth directions \hat{G} that entail minimal strain energy. Harmonic continuum elasticity theory^{2,3,4,5,6,7,8,9} makes definitive predictions for the a_s - and \hat{G} -dependence of epitaxial strain energy: (i) $q(a_s, \hat{G})$ does not depend on a_s , and (ii) the “softest direction” is $\langle 001 \rangle$ if $\Delta = [C_{44} - \frac{1}{2}(C_{11} - C_{12})] > 0$, while if $\Delta < 0$ then the softest direction is $\langle 111 \rangle$. For most fcc metals and semiconductors $\Delta > 0$, whereas $\Delta < 0$ for ionic salts (PbS, AgBr, NaCl, KCl) and several bcc metals (Nb, V, Mo, Cr). The selection of substrate orientation for many years has been guided by these predictions of harmonic elasticity, summarized compactly by the expression^{6,7}

$$q_{\text{harm}}(\hat{G}) = 1 - \frac{B}{C_{11} + \Delta \gamma_{\text{harm}}(\hat{G})}, \quad (2)$$

where $B = \frac{1}{3}(C_{11} + 2C_{12})$ is the bulk modulus and $\gamma_{\text{harm}}(\hat{G})$ is a purely geometric function of the spherical

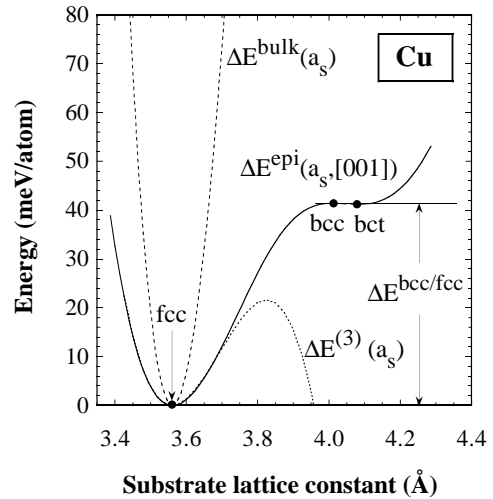


FIG. 1. Epitaxial ($\Delta E^{\text{epi}}(a_s, \hat{G})$, solid line) and hydrostatic ($\Delta E^{\text{bulk}}(a_s)$, dashed line) deformation energies for fcc Cu. The dotted line shows a fit to $\Delta E^{\text{epi}}(a_s, \hat{G})$ using 3-rd order polynomial in a_s .

angles formed by \hat{G} :

$$\begin{aligned} \gamma_{\text{harm}}(\phi, \theta) &= \sin^2(2\theta) + \sin^4(\theta) \sin^2 \\ &= \frac{4}{5} \sqrt{4\pi} [K_0(\phi, \theta) - \frac{2}{\sqrt{21}} K_4(\phi, \theta)]. \end{aligned} \quad (3)$$

$K_l(\phi, \theta)$ are Kubic harmonics¹⁰ (linear combinations of spherical harmonics forming irreducible representations of the cubic group), and the spherical angles ϕ and θ are measured with respect to Cartesian axes oriented along the edges of the conventional fcc cubic cell. Figures 2(b) and 2(c) show $q_{\text{harm}}(\hat{G})$ of Au and Cu, demonstrating that $\langle 001 \rangle$ and $\langle 111 \rangle$ are, respectively, the softest and hardest directions.

One expects to find corrections to the harmonic behavior predicted by Eq. (2) due to the fact that strong deformations may alter the electronic charge density (and thus, the elastic response) beyond the validity of conventional harmonic elasticity theory. However, the theory of elasticity itself does not indicate when and how expres-

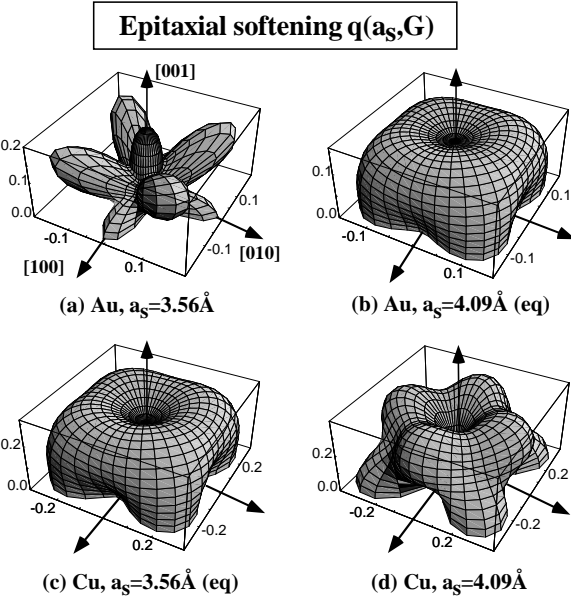


FIG. 2. Parametric plot of the epitaxial softening function $q(a_s, \hat{G})$ vs. substrate orientation \hat{G} for (a)–(b) Au and (c)–(d) Cu, at a few values of the substrate lattice constant a_s . The equilibrium (eq) lattice constants of fcc Au and fcc Cu are shown in (b) and (c), respectively.

sion (2) will fail for a given system. Figure 1 shows that at least a fourth-order polynomial in a_s is needed to reproduce the qualitative structure in $\Delta E^{\text{epi}}(a_s, [001])$ for Cu, as obtained directly from accurate electronic structure calculations (see below). The three extremal points in $\Delta E^{\text{epi}}(a_s, [001])$ suggest that a simple extension of the harmonic elasticity to include third-order elastic constants is not sufficient (the dotted line in Fig. 1 shows the behavior of the strain energy predicted by a 3-rd order polynomial fit to a few data points around $a_{\text{eq}} = 3.56 \text{ \AA}$). The goal of the present work is to propose a simple analytic formula for $q(a_s, \hat{G})$ [and therefore $\Delta E^{\text{epi}}(a_s, \hat{G})$] which works for arbitrary strain magnitude and direction \hat{G} .

We have calculated $\Delta E^{\text{epi}}(a_s, \hat{G})$ and $q(a_s, \hat{G})$ for Ag, Au, Cu and Ni along six principal directions $\langle 001 \rangle$, $\langle 111 \rangle$, $\langle 110 \rangle$, $\langle 113 \rangle$, $\langle 201 \rangle$ and $\langle 221 \rangle$ using the local density approximation (LDA),¹¹ as implemented by the linear augmented plane wave (LAPW) method.¹² This approach gives the total energy as a function of biaxial distortion, including all anharmonic effects. We find that our results can be fitted accurately to a generalization of the Kubic harmonic expansion of Eq. (3):

$$\gamma(a_s, \hat{G}) = \gamma_{\text{harm}}(\hat{G}) + \sum_{l=0}^{l_{\text{max}}} b_l(a_s) K_l(\hat{G}), \quad (4)$$

where $b_l(a_s)$ is now a function of a_s , and the angular momenta extended beyond the harmonic limit ($l = 0, 4$) to include $l = 6, 8, 10, \dots$. The analytic representation of Eq. (4) allows us to explore the elastically soft and elastically hard directions for *any* strain, even outside the regime of harmonic elasticity. We find that for *fcc* noble metals $q(a_s, [001])$ and $q(a_s, [111])$ soften as a_s expands (tensile strain) while $q(a_s, [110])$ and $q(a_s, [201])$ soften

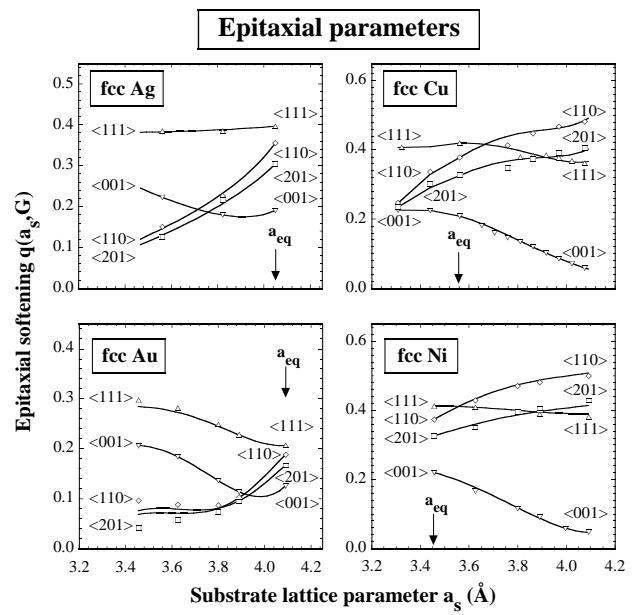


FIG. 3. The calculated epitaxial softening functions $q(a_s, \hat{G})$ vs. substrate lattice parameter a_s for Ag, Au, Cu and Ni. Points represent the directly calculated LDA values and lines show the fit using Eq. (4).

as a_s contracts (compressive strain). Consequently, upon sufficient compression $\langle 001 \rangle$ is no longer the softest direction, but rather $\langle 201 \rangle$ is (e.g., Ag, Au). Also, upon sufficient expansion, $\langle 111 \rangle$ is no longer the hardest direction, which is now $\langle 110 \rangle$ (e.g., Cu, Ni). Finally, the dramatic softening of $q(a_s, [001])$ upon biaxial expansion reflects the existence of low-energy “excited” bcc and bct crystal forms. These results can better guide the selection of substrate orientation for effective epitaxial growth.

We have performed LDA calculations for biaxial compression ($a_s < a_{\text{eq}}$) of Au and Ag, for biaxial expansion ($a_s > a_{\text{eq}}$) of Ni, while for Cu we considered both expansion and compression. Table I gives the calculated LDA elastic constants, which are typically 10–20% higher than the experimental values for Cu, Ag and Au. Larger discrepancy in the case of fcc Ni is due to the neglect of spin-polarization effects in our LAPW calculations. Figure 3 shows a line plot of $q(a_s, \hat{G})$ vs. a_s for a few directions \hat{G} , while Fig. 2 shows a parametric plot of $q(a_s, \hat{G})$ vs. \hat{G} for a few substrate lattice constants a_s . We find several surprising predictions relative to the expectations of harmonic elasticity. Although the harmonic expression $q_{\text{harm}}(\hat{G})$ [Eq. 2] is exactly satisfied at the equilibrium lattice constant $a_s = a_{\text{eq}}$ [where $\lim_{a_s \rightarrow a_{\text{eq}}} b_l(a_s) = 0$ in Eq. (4)], this ceases to be so as a_s deviates from a_{eq} . This is apparent from the dependence of q on a_s (absent in the harmonic theory), from the crossing of q for different \hat{G} values, and from the development of new lobes and minima in Fig. 2 with the change in a_s . Such effects occur at $\Delta a/a < 4\%$, suggesting a rather small range of validity of the harmonic approximation. Furthermore, in the harmonic elasticity theory, if $\langle 001 \rangle$ is the softest direction then $\langle 111 \rangle$ must be the hardest direction, and vice versa. Figure 3 shows that this does not hold for sufficiently deformed films: the hardest direction in Ni and

TABLE I. The calculated and experimental (Ref. 17) elastic constants of fcc Ag, fcc Au, fcc Cu and fcc Ni (in Mbar).

	Ag		Au		Cu		Ni	
	Calc.	Expt.	Calc.	Expt.	Calc.	Expt.	Calc.	Expt.
C_{11}	1.52	1.24	2.14	1.86	2.30	1.68	3.30	2.47
C_{12}	1.09	0.93	1.73	1.57	1.58	1.21	2.20	1.47
C_{44}	0.61	0.46	0.37	0.42	0.99	0.75	1.36	1.25

Cu for $a_s \gg a_{eq}$ is $\langle 001 \rangle$, while the hardest directions for Ag and Au at $a_s \ll a_{eq}$ are $\langle 111 \rangle$ and $\langle 001 \rangle$.

The new results for fcc noble metals, apparent from our self-consistent LDA calculations, are:

(i) $q(a_s, [001])$ and, to a lesser extent, $q(a_s, [111])$ soften as a_s expands (tensile biaxial strain).

(ii) $q(a_s, [110])$ and $q(a_s, [201])$ soften as a_s is compressed.

(iii) As a result of (i) and (ii) above, we find that upon sufficient compression, $\langle 001 \rangle$ is no longer the elastically softest direction, but $\langle 201 \rangle$ and, to a lesser extent, $\langle 110 \rangle$ are. The hardest direction upon compression is still $\langle 111 \rangle$.

(iv) Upon sufficient expansion, $\langle 111 \rangle$ is no longer the hardest direction, but $\langle 110 \rangle$ is (Cu, Ni). The softest direction upon expansion is still $\langle 001 \rangle$.

We find that result (i) is a reflection of the existence of a *low-energy* bcc and bct “excited” structures. Indeed, $\langle 001 \rangle$ strain applied to fcc lattice defines a Bain path,¹³ transforming fcc into bcc via the body-centered tetragonal structure. This intermediate structure is characterized by tetragonal unit cell dimensions a and c . When minimizing the total energy of a $\langle 001 \rangle$ biaxially deformed solid with respect to the out-of-plane lattice vector c at each in-plane lattice parameter a_s , one finds an “epitaxial $\langle 001 \rangle$ Bain path”¹⁴ (solid line in Fig. 1). For noble metals having the fcc structure ($c/a = \sqrt{2}$) at equilibrium, this deformation path contains the bcc ($c/a = 1$) saddle point, and the bct ($c/a = 0.96$ in the case of Cu) local minimum.^{14,15,16} The low amplitude of the epitaxial $\langle 001 \rangle$ Bain path relative to the hydrostatic path (Fig. 1) defines the softness of $q(a_s, [001])$ via Eq. (1), and therefore is a direct manifestation of the small fcc/bcc and fcc/bct energy differences. Indeed, the epitaxial softening function at $c/a = 1$ is given by

$$q(a_s, [001]) = \frac{\Delta E^{bcc/fcc}}{\Delta E_{fcc}^{bulk}(a_s)}, \quad (5)$$

where $\Delta E^{bcc/fcc} = E_{tot}^{bcc}(V_{eq}^{bcc}) - E_{tot}^{fcc}(V_{eq}^{fcc})$. Since in fcc noble metals $V_{eq}^{bcc} \approx V_{eq}^{fcc}$, the bcc point is reached at $a_s \approx 2^{\frac{1}{3}}a_{eq}$ (see Fig. 3).

A similar argument explains the softening of $q(a_s, [111])$, since the epitaxial $\langle 111 \rangle$ Bain path also connects cubic fcc ($c/a = \sqrt{6}$) and bcc ($c/a = \sqrt{6}/4$) structures.¹⁵ This property of the $\langle 001 \rangle$ and $\langle 111 \rangle$ Bain paths is caused by the cubic symmetry of the crystal at the bcc point $c/a = 1$, requiring it to be a local extremum of the total energy. It is interesting that in zincblende solids (two interpenetrating fcc lattices), tetragonal $\langle 001 \rangle$ expansion does not lead to an extremal

point in $\Delta E^{epi}(a_s, [001])$ since the crystal at the “bcc point” $c/a = 1$ does not possess higher symmetry than at $c/a \neq 1$. As a consequence, $\Delta E^{epi}(a_s, [001])$ is a monotonically increasing function of a_s , and $\langle 001 \rangle$ tensile strain does not lead to a softening of $q(a_s, [001])$.

The consequences of our findings are as follows: (a) Films of fcc noble metals under *tensile* biaxial strain possess the lowest strain energy for strain direction $\langle 001 \rangle$, while large *compressive* biaxial strains will have lower strain energy for $\langle 201 \rangle$. (b) When growing an S_pL_q superlattice with components having small (S) and large (L) lattice constants (e.g., $S = Cu$, $L = Au$), the system rich in L ($q \gg p$) will have a low $\langle 001 \rangle$ elastic strain energy due to easy expansion of S , while a system rich in S ($q \ll p$) will have a low $\langle 201 \rangle$ elastic energy due to easy compression of L .

This work has been supported by the Office of Energy Research, Basic Energy Sciences, Materials Science Division, U.S. Department of Energy, under contract DE-AC36-83CH10093.

¹ For recent advances in heteroepitaxy see M. H. Francombe, J. Vac. Sci. Technol. A **12**, 928 (1994); J. R. Arthur, Surf. Sci. **299/300**, 818 (1994); H. Lüth, Surf. Sci. **299/300**, 867 (1994); F. Capasso and A. Y. Cho, Surf. Sci. **299/300**, 878 (1994).

² J. Hornstra and W. J. Bartels, J. Cryst. Growth **44**, 513 (1978).

³ E. Anastassakis, J. Appl. Phys. **68**, 4561 (1990); J. Cryst. Growth **114**, 647 (1991).

⁴ D. M. Wood and A. Zunger, Phys. Rev. Lett. **61**, 1501 (1988); Phys. Rev. B **38**, 12 756 (1988); Phys. Rev. B **40**, 4062 (1989).

⁵ D. M. Wood, J. Vac. Sci. Technol. B **10**, 1675 (1992), and references therein.

⁶ D. B. Laks, L. G. Ferreira, S. Froyen, and A. Zunger, Phys. Rev. B **46**, 12 587 (1992).

⁷ A. Zunger, in *Handbook of Crystal Growth*, Vol. 3, edited by D. T. J. Hurle (Elsevier, Amsterdam, 1994), p. 997.

⁸ P. M. Marcus and F. Jona, Phys. Rev. B **51**, 5263 (1995).

⁹ D. J. Bottomley and P. Fons, J. Cryst. Growth **160**, 406 (1996).

¹⁰ A. L. Altman and A. P. Cracknell, Rev. Mod. Phys. **37**, 19 (1965).

¹¹ P. Hohenberg and W. Kohn, Phys. Rev. **136**, 864 (1964); W. Kohn and L. J. Sham, Phys. Rev. A **136**, 1133 (1965).

¹² S.-H. Wei and H. Krakauer, Phys. Rev. Lett. **55**, 1200 (1985), and references therein.

¹³ E. C. Bain, Trans. Am. Inst. Min. Metall. Eng. **70**, 25 (1924).

¹⁴ P. Alippi, P. M. Marcus, and M. Scheffler, Phys. Rev. Lett **78**, 3892 (1997).

¹⁵ T. Kraft, P. M. Marcus, M. Methfessel, and M. Scheffler, Phys. Rev. B **48**, 5886 (1993).

¹⁶ P. J. Craievich, M. Weinert, J. M. Sanchez, and R. E. Watson, Phys. Rev. Lett. **72** 3076 (1994).

¹⁷ H. B. Huntington, in *Solid State Physics*, eds. F. Seitz and D. Turnbull (Academic Press, New York, 1958), p. 274.